Journal of Applied Electrochemistry (2006) 36:347–353
DOI 10.1007/s10800-005-9070-2

Pitting corrosion of Cr–Mn–N steel in sulphuric acid media

B.R. TZANEVA[1,*], L.B. FACHIKOV[2] and R.G. RAICHEFF[2]
[1]*Department of Chemistry, Technical University, FETT, 8 Kliment Ohridsky Blvd., 1756, Sofia, Bulgaria*
[2]*University of Chemical Technology and Metallurgy, Sofia, Bulgaria*
*(*author for correspondence, e-mail: borianatz@tu-sofia.bg)*

Received 30 September 2004; accepted in revised form 13 September 2005

Key words: chloride ions, manganese, nitrogen, pitting corrosion, stainless steel, sulphuric acid

Abstract

The resistance to pitting corrosion of austenitic stainless steel Cr18Mn12N has been studied in model solutions of sulphuric acid (0.5 M) containing chloride ions (0.5 M). The cyclic potentiodynamic method has been employed to investigate the effects of chloride ions and agitation rate on the pitting and repassivation potentials. Electron and optical microscopy, electron diffraction spectroscopy and atomic absorption spectrometry have been used to detect the surface sites for pit formation and the growth of pit nuclei. The results obtained with chromium–manganese–nitrogen steel have been compared with those of austenitic Cr18Ni9 stainless steel. A similarity in pit initiation is established, while steel composition exhibits no significant effect. Cr18Mn12N steel is less prone to repassivation as compared with Cr18Ni9 steel.

1. Introduction

The incorporation of nitrogen in steel is a new trend in the field of ferrous alloys. Numerous nitrogen containing stainless steels with different nitrogen content have been reported: classical Cr–Ni steels with incorporated nitrogen [1–6], Cr–Ni steels with reduced nickel content, partially or fully replaced by austenite forming elements, more frequently manganese, etc. [3].

The studies of the pitting corrosion of nitrogen containing steels have led to the formulation of different hypotheses [7].

All emphasize the positive effect on steel resistance by the accumulation of nitrogen at the steel surface. However the question as to how nitrogen segregates at the steel surface is still open. According to Olefjord and Wegrelius [8] nitrogen, similarly to nickel, accumulates at the interphase boundary metal/oxide and its concentration increases with increase in both the applied potential and the polarization time. Other authors consider [8–10] that nitrogen is in the elemental state, while others suggest that it is in the form of surface nitrides [11, 12]. Despite these differences the positive effect of nitrogen on the stability of the passive state of steels is confirmed. Moreover, a relationship between the surface segregation of nitrogen and enrichment of the passive film with Cr^{3+} has been established [11].

Manganese as an alloying element of steels has been studied mainly due to the formation of anodic non-metallic inclusions of manganese sulphide, the latter being the preferred sites for pit nucleation [2, 13]. The alloying of steel with manganese under these studies is relatively low (up to 2%) and the results indicate its negative effect on the alloy resistance against pitting corrosion. On the other hand, similar studies on steels with high manganese content [6, 14] also confirm its promoting effect on the pit initiation.

Some authors have studied the effect of agitation of the corrosive media on passivity breakdown. According to Tchechovsky and Burian [15] the fluid flow retards the pit nucleation due to the reduction of the surface concentration of the aggressive ion. Sato et al. [16] have performed experiments with a rotating stainless steel disc electrode, but significant changes in the frequency of pits and pitting potential with variations of disc rotation speed have not been detected. On the other hand, Harb and Alkire [17] have demonstrated that fluid flow is the strongest factor affecting the pit growth. They have developed a model of hemispherical pits not covered by a film; according to this model, the pit dissolution rate depends on the potential only. The electrolyte stirring could repassivate the pits by reduction of solution concentration inside the pits. In some cases, however, a reverse effect can be observed associated with the inhibition of salt film formation [18]. Beck and Chan [19] reported that the effect of agitation rate on the repassivation of pits is mainly due to destruction of the salt film.

Sulphuric acid aqueous solutions containing chlorides are frequently employed in the study of stainless steel

passivation behaviour [1, 13, 20, 21], since they ensure combined action of the aggressive medium (low pH) with high reproducibility of the characteristic parameters of pitting corrosion (the pitting potential E_{pit}, the repassivation potential E_{rp}), thus providing almost the best conditions for testing new materials.

The present work reports the results of a pitting initiation and repassivation study of Cr18Mn12N steel in 0.5 M sulphuric acid solution without and with 0.5 M sodium chloride. Special attention is paid to the effect of solution stirring on pitting potential and pit shapes. The pitting behaviour of chromium–manganese–nitrogen steel is compared with that of the austenitic Cr18Ni9 steel.

2. Experimental details

The chemical composition of the steels studied is shown in Table 1. The austenitic microstructures of both steels were obtained by quenching in water after heating at 1100 °C. Oxides and oxide–sulphides were mainly detected as non-metallic inclusions in the steels. The chromium–manganese–nitrogen steel contains more inclusions than the chromium–nickel steel and the main inclusions are sulphides and, to a lesser extent, nitrides and oxides.

The electrodes were disks with 0.5 cm^2 working surface. At the beginning of the electrochemical tests, the samples were treated in the following sequence: (i) manual finishing with 600 grit abrasive paper; (ii) passivation in a bath of nitric acid (1:1) for 10 min (to exclude crevice corrosion); (iii) second polishing just before the test with 800 grit abrasive paper; (iv) rinsing with distilled water and (v) degreasing with an alcohol–ether mixture. The test corrosive media – 0.5 M sulphuric acid and 0.5 M sulphuric acid containing 0.5 M sodium chloride – were prepared using analytical grade reagents and distilled water. The tests were performed under open air conditions at room temperature (20 °C).

The *cyclic polarization pitting test* is a relatively rapid technique that allows the study of the pitting resistances of numerous alloys. The pitting potential (E_{pit}) and the repassivation potential (E_{rp}) were determined and used to characterize the steel resistance against pitting corrosion. The electrochemical investigations were carried out in a conventional three-electrode cell with a platinum counter electrode and a saturated calomel reference electrode (SCE). The measurements were performed with a PAR-263 potentiostat and M352 Soft Corr Corrosion Measurement and Analysis Software. In the potentiodynamic tests, the specimens were first cathodically polarized to −700 mV (SCE) and kept for 1 min under these conditions, followed by anodic polarization carried out at a potential scan rate 1 mV s^{-1} in the positive direction up to 10^{-4} A cm^{-2} current density. The polarization in the reverse (negative) direction was carried out down to the point where the curve intersected the anodic curve in the passive region.

Table 1. Chemical compositions of steels tested (%wt)

Steel	Cr	Mn	Ni	Si	N	C
Cr18Mn12N	16.5	12.00	–	0.30	0.61	0.04
Cr18Ni9	17.49	1.28	9.37	0.52	–	0.055

The rotation speed of the disc electrode was changed within in the range 0–2000 rpm. The steady state polarization curves were traced in the test solution with chloride ions. The potentiodynamic method was applied at various rotation speeds in order to obtain a set of anodic polarization curves.

The microstructure of both steels and the type of the corrosion attack were determined by optical (Epityp-2) and electron (JEOL) microscopy.

Energy dispersive spectroscopy (EDS) (VG Ma500 Auger microscope) and atomic absorption spectrometry (AAS) (Perkin Elmer 3030) were used to analyse the surfaces attacked by pitting corrosion and the products in the corrosive media. For this purpose the steel samples with polished surface were treated galvanostatically for 12 h in a 0.5 M sulphuric acid solution containing 0.5 M sodium chloride under anodic current density of 1.2×10^{-4} A cm^{-2}. Both the high current density and the duration of the polarization offered a possibility for large pits to form. These conditions also yield high concentrations of metal ions in the solution provided mainly by the pit cavities.

3. Results and discussion

3.1. *Study of pitting corrosion by the potentiodynamic method*

Under anodic polarization the samples of austenitic stainless steels (in 0.5 M sulphuric acid solution) acquired a passive state, with breakdown at the transpassivity potential – about 900 mV (SCE) (Figure 1). The parameters characterizing anodic passivity (the passivation current density and the passivating potential) for both steels are identical and the widths of the passive region are almost equal, which is an indication for similarity of the passive films formed on the metal surfaces under these conditions.

The addition of chloride ions to the sulphuric acid solution leads to a sharp current increase at potentials significantly lower than those of transpassivity (Figure 1). The current increase is caused by the breakdown of the passive film and development of pitting corrosion. The passive film perforation yields a narrow range of potentials corresponding to the passive state – about 600 mV for Cr18Mn12N and 500 mV for Cr18Ni9 steel. The plots in Figure 1 demonstrate similar anodic behaviour of both steels, within the passive state range, regardless the absence (curves 3 and 4) and presence (curves 1 and 2) of chloride ions. This fact may be attributed to the similarity of the passive films. The replacement of nickel by manganese and nitrogen obviously does not significantly

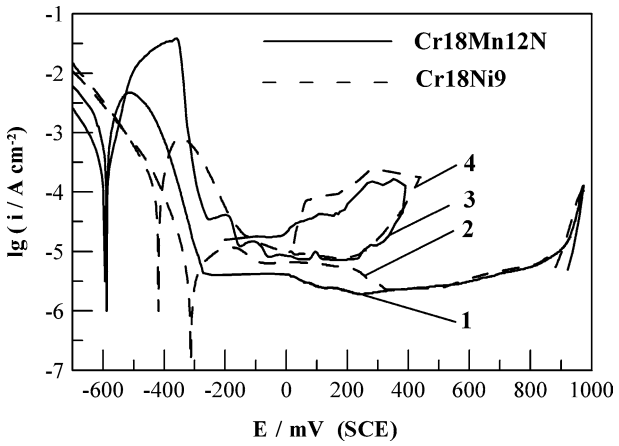

Fig. 1. Polarization curves of Cr18Mn12N and Cr18Ni9 steels at 20 °C, scan rate 1 mV s^{-1}: curves 1 and 2 – in 0.5 M sulphuric acid solution; curves 3 and 4 – in 0.5 M sulphuric acid solution containing 0.5 M sodium chloride.

affect the initial stage of pit nucleation in sulphuric acid media.

The reverse shift of potential in the cathodic direction (100–200 mV) leads to an initial current increase attributed to the sustainable development of pits. With a further shift of potential in the same direction the repassivation potential (E_{rp}) is reached when the passive film and its protective properties are restored.

When the sulphuric acid solution contains chloride ions, the potentiodynamic method demonstrates a better repassivation capability of the classical chromium–nickel steel as compared to chromium–manganese–nitrogen steel. The plots in Figure 1 show that Cr18Mn12N steel exhibits a difference between E_{pit} and E_{rp} larger than that of Cr18Ni9 steel. Similar results concerning the repassivation properties of the steels studied (under different experimental conditions) were also reported earlier [22, 23]. The difference between the repassivation ability of both steels can be explained by their different compositions. The absence of nickel and the higher manganese content in the chromium–manganese–nitrogen steel reduce its repassivation ability after breakdown of the protective film.

Figure 2 shows the change in pitting and repassivation potentials vs. electrode rotation speed. The agitation of the electrolyte affected significantly processes associated with the passive state breakdown on the steel surface. The pitting potentials of the steels had quite similar values and became more positive as the electrode rotation speed was increased. In the case of Cr18Mn12N steel, the shift of E_{pit} in the positive direction was linear in the within the range 0–2000 rpm, whereas for the Cr18Ni9 steel it was observed only at around 1000 rpm which is in accordance with the literature [10, 12].

Increase in rotation speed of the disk electrode led to a slight shift (50–80 mV) of the repassivation potential (E_{rp}) towards more positive values for chromium–manganese–nitrogen steel, while the shift for chromium–nickel steel was larger (more than 120 mV).

3.2. *Microscopic studies*

The optical and SEM observations of the samples after exposure in 0.5 M H_2SO_4 solution indicated that the medium did not provoke local changes of the surface, while the addition of chlorides developed pitting corrosion. The number of pits formed on the surface of the chromium–manganese–nitrogen steel is relatively small, but they are deeper. The pits observed on the surface of the Cr18Mn12N steel are irregular (Figure 3a, b) or hemispherical open cavities, while those on the surface of the classical austenitic steel are mainly covered cavities (Figure 4a).

The microscopic studies of Cr18Mn12N surfaces affected by pitting corrosion indicate that corrosion attack is located around the non-metallic inclusions (Figure 3). The pits observed on the classical chromium–nickel steel grow not only around such non-metallic inclusions, but also upon surface defects. A more characteristic example of pit formation at the boundary of three grains is illustrated in Figure 4b (the contacting grains are well observed at the cavity bottom).

The weak repassivation ability of Cr18Mn12N (as determined by the potentiodynamic method) can be also explained by the results above mentioned. The anodic non-metallic inclusions (manganese sulphide) retain the local anodes in active state [13]. The dissolution of inclusions stimulates the penetration of pits into the steel, leading to a significant change in the chemical composition of the electrolyte inside the cavity. Generally, the latter is affected by hindered ion exchange between the solution in the cavity and in the bulk, as well as by the accumulation of ions (mainly Mn^{2+} and S^{2-}) due to dissolution of the non-metallic inclusions. Moreover, the repassivation of the pits developed on Cr18Mn12N steel surfaces is suppressed by the high manganese content which hinders the positive effect of nitrogen. To the best of our knowledge no reported results for the effect of manganese on repassivation exists; however, its high activity and the negative effect on passivity [2, 14] suggest that the lower corrosion resistance of the new austenitic

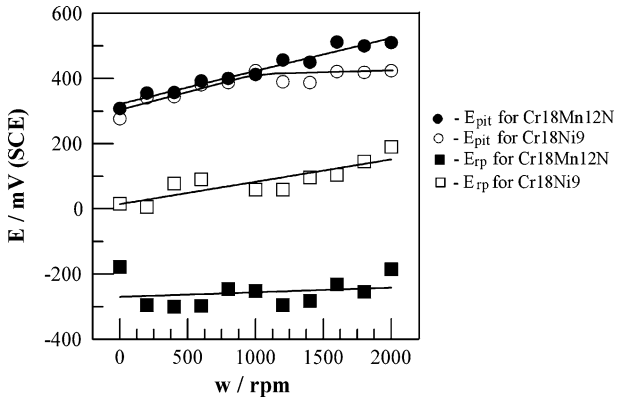

Fig. 2. Pitting and repassivation potentials of Cr18Mn12N and Cr18Ni9 steels determined by cyclic polarization tests vs. disk rotation speed in 0.5 M sulphuric acid solution containing 0.5 M sodium chloride at 20 °C.

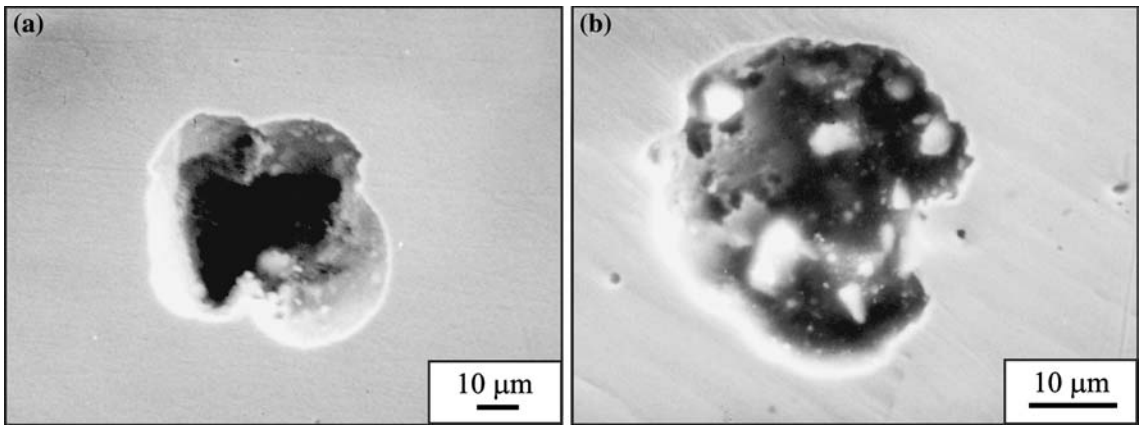

Fig. 3. SEM micrographs of pits formed on Cr18Mn12N steel.

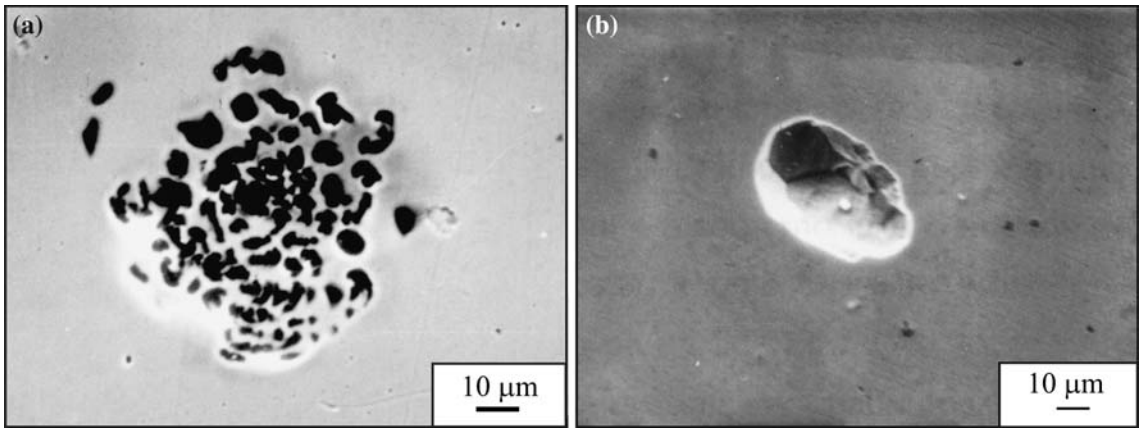

Fig. 4. SEM micrographs of pits formed on Cr18Ni9 steel.

steel can be attributed to the high content of this alloying element.

Electrolyte agitation leads to an increase in the average size and to a decrease in the maximum size of pits. The latter can be related to the enhanced repassivation ability of the open pits (Cr18Mn12N samples) by the rotation of the disk which allows nucleation of new pits near the repassivated ones. The difference in the size of small and large pits on Cr18Ni9 increases as agitation intensity increases. The latter also changes the type of pits: at higher agitation intensity, more pits have open cavities. This is in disagreement with the results of Lacome [24] for AISI 304 steel who assumed that agitation hindered the destruction of the lacy metallic cover of pits.

An interesting result obtained here is that under intensive agitation of the solution (above 1600 rpm) both steels demonstrate similar pitting corrosion behaviour.

The increase in the repassivation ability at increased disk rotation speed can be explained by the enhanced oxygen supply which favours repassivation as well as by the open shape of pits which allows immediate repassivation after decrease in anodic polarization.

3.3. *Energy dispersive spectroscopy (EDS)*

Results of EDS of the sample surfaces (Cr18Mn12N steel) attacked by pitting corrosion are summarized in Figure 5 and Table 2. The method was used to study the passive surface, i.e. non-affected by the pits (Figure 5a) as well as the bottoms of three typical pits (Figure 5b–d).

The pit P-1 (Figure 6a) has small size ($d \approx 4.4\ \mu m$) with a circular opening and is relatively deep with respect to its surface diameter. Its bottom contains an increased amount of manganese while weak peaks of sulphur and chloride are recorded (Figure 5b). The low S content indicates that the initial destruction of the surface starts by dissolution of a non-metallic manganese sulphide inclusion, the latter being completely dissolved due to the lasting anodic polarization. The SEM micrograph of this pit shows some light spots at the bottom indicating the presence of salt film deposits. Further development of the pit in depth gives a dark spot at the bottom that can be attributed to further dissolution of the steel confirmed by the peaks of chromium and iron in the EDS spectra. Data in Table 2 show that the solution inside the pit was more aggressive towards iron than to chromium. The long

lasting pit growth could lead to the accumulation of chromium and to competition between the activating action of the salt film and the repassivation action of chromium.

The second type of pitting P-2 (Figures 5b and 6b) is larger ($d \approx 28\ \mu m$) than P-1. During the initial stage the pit cavity was covered, but in the course of its growth an open cavity was formed. The changes in the solution content inside the cavity are similar to those already reported for pit P-1; however the chromium content is lower than that on the passive surface. At the left side of the cavity bottom a porous structure (probably a salt film) is observed, while in the lower part of the cavity the corrosion attack penetrates deeper. The right side of the cavity contains a crystal structure area that may be due to a non-metallic inclusion (the spectrum displays a relatively high silicon peak).

The light area around the mouths of pits P-1 and P-2 indicates the presence of salt films deposited during the initial dissolution stages of manganese sulphide inclusions prior to the formation of deep cavities. According to Baker and Castle [13], sulphide anions preferably pass into solution in the course of manganese sulphide dissolution, while manganese ions remain in the cavity and consequently attract and capture significant amounts of chloride ions. In the course of the process a salt film is deposited in the cavity bottom maintains retains the pit in the active state. Salt film formation is enhanced, facilitated also by the relatively large pitting cavities (the depth surpasses the mouth diameter). This pit geometry hinders ion exchange between electrolyte in the pit and in the bulk and favours attainment of the critical electrolyte concentration for salt precipitation. In the volume of pit P-2 the salt deposition process is further enhanced by the partly covered shape of the cavity at the initial stage resulting in a deep corrosion attack. The salt film has high ohmic resistance and the steel base dissolves in active state. Under similar conditions all the three

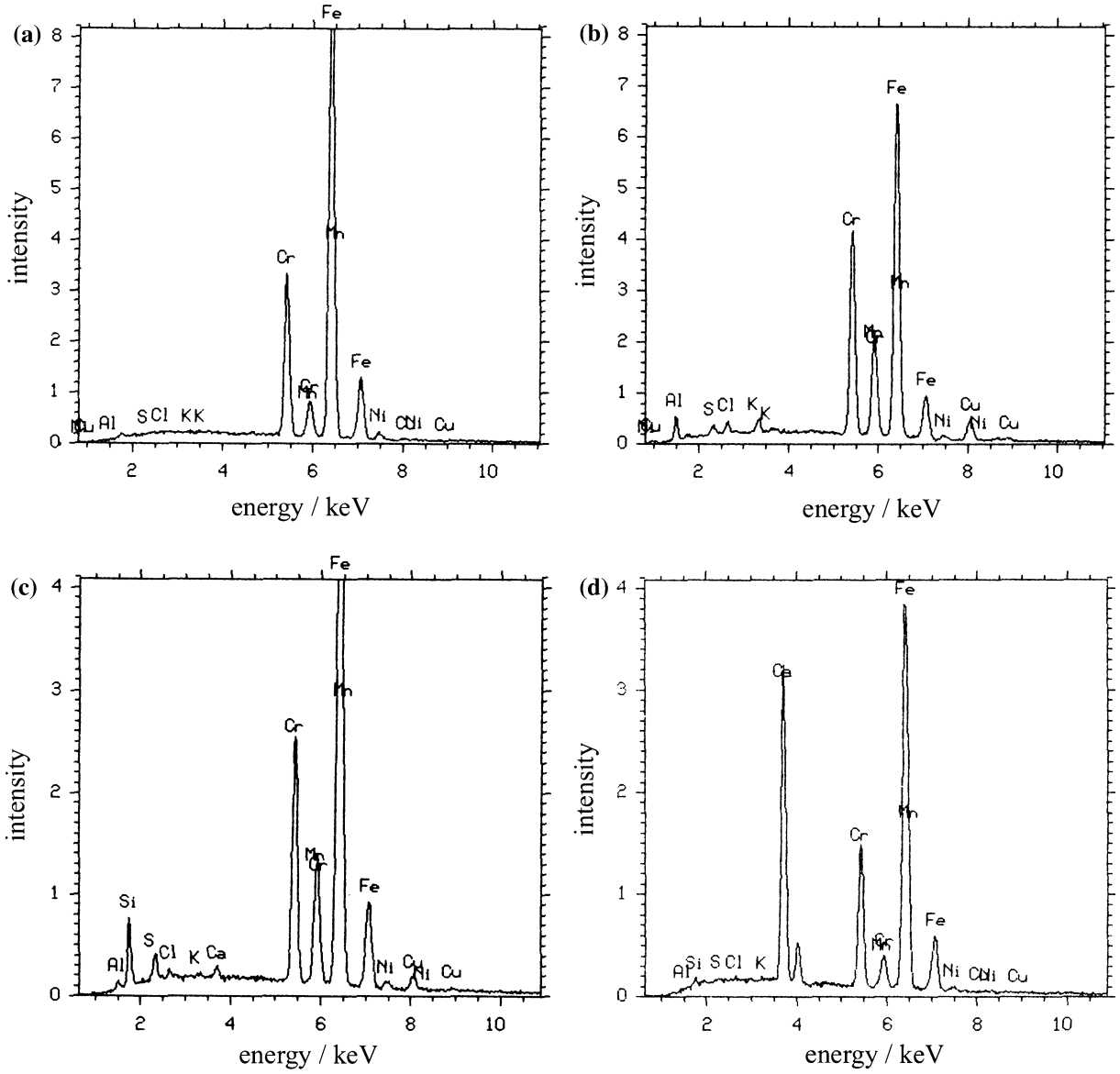

Fig. 5. EDS spectra of different sections of the Cr18Mn12N sample surface after development of pitting corrosion: (a) passive surface; (b–d) pits P-1, P-2 and P-3.

Table 2. Energies of characteristic peaks of EDS spectra and ratios of spectral intensities at the pit's bottom (I') and the passive surface (I'')

Element	Energy/ keV		Ratios for different pits		
			P-1	P-2	P-3
Fe	7.07	$\frac{I'_{Fe}}{I''_{Fe}}$	0.73	0.73	0.43
Cr	5.42	$\frac{I'Cr}{I''_{Cr}}$	1.24	0.76	0.44
Mn (mixed with Cr)	5.91	$\frac{I'_{Mn}}{I''_{Mn}}$	2.75	1.62	0.5

alloying elements of steel can be dissolved, but the contribution of manganese is more pronounced (due to its higher electrochemical activity), followed by chromium and iron. The main amount of dissolved manganese remains in the pit cavity, while chromium and iron pass into the bulk electrolyte. The concentration of manganese ions in the cavity increases, thus supporting the formation of salt films at the bottom. This autocatalytic process enhances pit growth in depth.

The above mentioned comments lead to the conclusion that the increased content of manganese in the pits is due to dissolved manganese sulphide inclusions and its high content in steel. Due to its high activity, manganese dissolves. Its exceptionally high amount in the pits is due to its participation in the salt film as a main cation, or to the precipitation of the solution in the pit after removing the sample from the corrosion test medium or to both reasons.

The third pit P-3 (Figures 5d and 6c) has an open structure ($d \approx 12\,\mu m$) with relatively small depth. The EDS spectrum indicates a reduced amount of the basic elements of the alloy (iron, chromium and manganese). The exceptionally low Cr content at the pit bottom (Table 2) contradicts the traditional viewpoints concerning the role of Cr as the main alloying element giving good protective properties of stainless steel surfaces. The low chromium content in the shallowest pit can be attributed to its reduced content in the metal phase underneath the oxide. It should be noted that the highest stability constant of chromium chloride complexes as compared to that of iron and manganese may facilitate chromium removal from steel [25].

It may be concluded that relatively deep pits on the surface of Cr18Mn12N steel are formed after the complete dissolution of the anodic inclusions (manganese sulphide). Inside the pit, the deposition processes mainly involve manganese (from the steel and inclusions) and anions from the electrolyte, the latter stimulating the corrosion attack in depth. On the other hand, the growth of open and shallow pit cavities depends mainly on the dissolution rates of the basic alloy elements.

The elucidation of the reason for the low chromium content detected at the bottoms of pits P-2 and P-3 should take into account that the decreased concentration of this element was recorded with respect to the content of the passive surface (chromium enriched). The same is valid for manganese whose unexpected high amounts at the bottom of pits P-1 and P-2 are related to the relative character of the measuring method. Therefore, the real variation of the elements cannot be detected by this method only and an analysis of the corrosive medium may provide additional information.

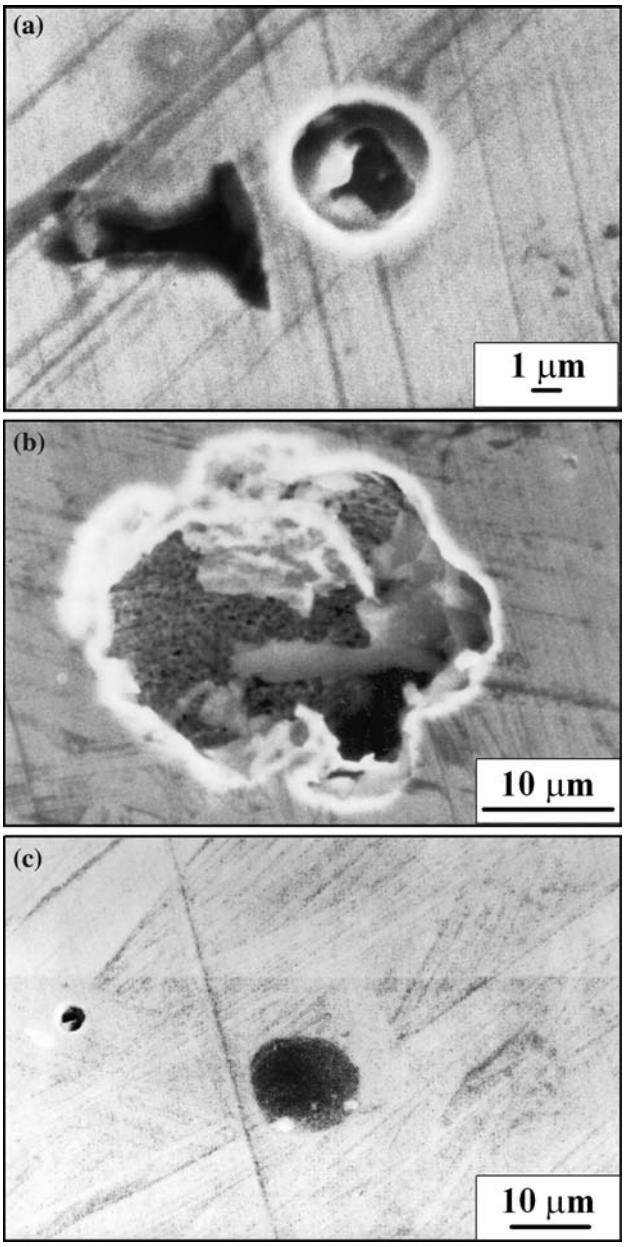

Fig. 6. SEM micrographs of pits formed on Cr18Mn12N steel and analyzed by EDS. (a–c) pits P-1, P-2 and P-3.

3.4. *Atomic absorption spectrometry*

The ratios of the content of the main elements (Fe, Cr, Mn and Ni) in the test solution ($\%M^{n+}$) and its content in steel (%M) are listed in Table 3. The content (%wt) of solutions and in steel is calculated for the main elements, while the content of the other elements is neglected. When the ratio $\%M^{n+}/\%M$ is less than one, this is indicative of the passing of element M in the solution in less degree, than is its quantity in steel, therefore the metal surface is

Table 3. Ratios of the content (%) of the main elements in the solution of 0.5 M H_2SO_4 + 0.5 M NaCl (after corrosion test at E_{corr} and E_{pit}) and in Cr18Mn12N and Cr18Ni9 steel

		Fe	Cr	Mn	Ni
Cr18Mn12N	After corrosion at E_{corr}	0.95	1.36	0.78	–
	After corrosion at E_{pit}	0.87	1.47	1.09	–
Cr18Ni9	After corrosion at E_{corr}	1.02	0.95	–	0.91
	After corrosion at E_{pit}	0.98	1.62	–	0.01

enriched with it. It is obvious from the Table 3 that at E_{corr} for steel Cr18Mn12N Cr dissolves most, the Fe less, and Mn to the smallest degree. The quantity of the last two elements in the solution is less than that in the steel. The results, obtained for steel Cr18Ni9 show that at the corrosion potential, the solution enriches approximately proportionally with Fe, Cr and Ni.

The quantity of these elements in the corrosion environment after pitting development can be presumed to result only from dissolution of steel in the pits, because the of the rest of the surface is passive. The analyzed solutions, obtained after galvanostatical polarization at $E > E_{pit}$, are enriched mainly with Cr and less with Fe. For Cr18Mn12N steel a slow increase in the Mn content in comparison with its content in steel is noted. It is unconditionally proved for Cr18Ni9 steel that under anodic potentials Ni does not dissolve.

4. Conclusions

1. Pitting corrosion of Cr18Mn12N and Cr18Ni9 steels in sulphuric acid media occurs only in the presence of chloride ions. The replacement of nickel by manganese and nitrogen does not affect the initial stage of pit growth, but hinders the repassivation properties of steel.
2. The corrosion attack on the surface of Cr18Mn12N steel is mainly located on the non-metallic inclusions and the pits grow as open cavities. The pits on Cr18Ni9 steel from at surface defects and the cavities are covered.
3. Agitation of the electrolyte hinders pit initiation and facilitates repassivation. At disk rotation speeds above 1600 rpm the character of the pitting corrosion for both Cr18Mn12N and Cr18Ni9 steels is similar.
4. The EDS and AAS analyses of Cr18Mn12N steel and of test solutions show that deep pits are formed after dissolution of the non-metallic inclusions (manganese sulphide). This dissolution process mainly affects manganese; most of the manganese ions remain inside the pits (in the salt film deposited at bottom of the cavity and in the pit electrolyte). Chromium shifts to the bulk solution.

References

1. S.J. Pawel, E.E. Stansbury and C.D. Lundin, *Corrosion* **45**(2) (1989) 125.
2. V. Mitrovic-Scepanovic and R.J. Brigham, *Corrosion* **52**(1) (1996) 23.
3. S. Ahila, B. Reynders and H. Grabke, *Corros. Sci.* **38**(11) (1996) 1991.
4. U. Kamachi Mudali, P. Shankar, S. Ningshen, R.K. Dayal, H.S. Khatak and B. Raj, *Corros. Sci.* **44**(10) (2002) 2183.
5. H. Baba, T. Kadama and Y. Katada, *Corros. Sci.* **44**(10) (2002) 2393.
6. Y.S. Lim, J.S. Kim, S.J. Ahn, H.S. Kwon and Y. Katada, *Corros. Sci.* **43**(1) (2001) 53.
7. R. Levey and A. van Bennekom, *Corrosion* **51**(12) (1995) 911.
8. I. Olefjord and L. Wegrelius, *Corros. Sci.* **38**(7) (1996) 1203.
9. R. Bandy and D. van Rooyen, *Corrosion* **41**(4) (1985) 228.
10. Y.C. Lu, R. Bandy, C.R. Clayton and R.C. Newman, *J. Electrochem. Soc.* **130**(8) (1983) 1774.
11. C. Clayton and K. Martin, *Evidence of Anodic Segregation of Nitrogen in High-Nitrogen Stainless Steels and Its Influence on Passivity*. (HNS 88 – The Institute of Metals, London, England, 1989), 256 pp.
12. R.D. Willenbruch, C.R. Clayton, M. Oversluizen, D. Kim and Y. Lu, *Corros. Sci.* **31** (1990) 179.
13. M.A. Baker and J.E. Castle, *Corros. Sci.* **34**(2) (1993) 667.
14. Y. Zhang and X. Zhu, *Corros. Sci.* **41**(9) (1999) 1817.
15. A. Tchechovsky and E. Burian, *Electrochemistry* **26**(12) (1990) 23 (Russia).
16. N. Sato, T. Nakagawa, K. Kudo and M. Sakashita, *in* R. Staehle, B. Brown, J. Kruger and A. Agrawal (Eds), 'Localized Corrosion', (NACE, Houston, Texas, 1974) p. 447.
17. J.N. Harb and R.C. Alkire, *J. Electrochem. Soc.* **138**(12) (1991) 3568.
18. R.C. Alkire and A. Cangellari, *J. Electrochem. Soc.* **130**(6) (1983) 1252.
19. T. Beck and S. Chan, *Corrosion* **37**(11) (1981) 665.
20. T.M.C. Nogueira and O.R. Mattos. Use of a rotating disc electrode to study the influence of sulphate anions on the anodic dissolution of iron, *in* M. Duprat (Ed.), *Electrochemical Methods in Corrosion Research* Vol. 8, (Materials Science Forum, Trans Tech Publications Ltd., Switzerland, 1986), pp. 43–52.
21. S. Haupt and H.-H. Strehblow, *Corros. Sci.* **37**(1) (1995) 43.
22. L. Fachikov, B. Borissova, R. Raicheff and V. Mikhnev, 'Corrosion behaviour of austenitic Cr–Mn–N–Steel in chloride medium', proceedings of the EUROCORR'97, Throndheim, Norway, 22–25 September (1997) 417.
23. B. Borissova, L. Fachikov and R. Raicheff, 'Corrosion behaviour of austenitic Cr–Mn–N steel in chloride medium: Influence of solution concentration and agitation', proceedings of the VIIth International Corrosion Symposium, Istanbul, Turkey, 18–20 October (2000) 120.
24. I. Lacome, 'Etude statistique par analyse d'images numerisees de la corrosion par piqures d'un acier inoxydable type A.I.S.I.304 en milieu chlorure', Dissertation (INP Toulouse, France, 1994).
25. B.P. Nikolsky (ed.), *Handbook of Chemist*. Vol. 3 (Himiya, Moskow, 1964) 124 pp.